Int. J. Solids Structures Vol. 21, No. 2, pp. 207–223, 1985
Printed in the U.S.A.

0020–7683/85 $3.00 + .00
Pergamon Press Ltd.

CYCLIC THERMAL LOADING IN THE CREEP RANGE—II. HIGH LEVELS OF THERMAL LOADING

A. C. F. COCKS
Department of Theoretical and Applied Mechanics, University of Illinois at Urbana-Champaign, Urbana, IL 61801, U.S.A.

AND

A. R. S. PONTER
Department of Engineering, Leicester University, Leicester LE1 7RH, England

(*Received* 18 *October* 1983; *in revised form* 7 *May* 1984)

Abstract—An upper displacement bound is presented for thermal loading problems that allows energy to be dissipated as a result of the cyclic variation of strain in parts of the structure. Use of the bound requires a knowledge of the thermo-elastic stress distribution resulting from the cycle of temperature and arbitrary stress fields that are in equilibrium with the primary load and a dummy load applied in the direction of the required displacement rate. Certain limitations are imposed on the choice of equilibrium stress fields and, as a result, the bound can only be applied to a limited range of problems. Situations for which the bound can and cannot be used are examined.

The bound is used to obtain a solution for the plate problem originally analysed by Bree [10]. The results are compared with the calculations of O'Donnell and Porowski [11] who adopt a different material model.

1. INTRODUCTION

In an accompanying paper [1] upper bounds on the deformation rate were derived for structures subjected to low levels of thermal loading for a material that deformed according to the Bailey-Orowan theory of creep [2]. This material model was chosen as opposed to a non-linear viscous model because it gave the more severe structural behaviour under cyclic loading conditions. Tests on simple two bar structures of Copper [3] and 316SS [4] also indicate that the recovery model gives the better prediction of experimental results. In these experiments the stresses remained tensile throughout the duration of the tests and the effects of reverse cycling were not investigated.

When a structure is subjected to high levels of thermal loading reversed plastic straining occurs in parts of it. Material behaviour under reversed loading conditions has received a lot of attention over the past few years [5], but no unified material model that lends itself to simplified analysis has yet emerged. With the present state of knowledge it seems pertinent to use the material model that predicts the most severe response of the structure when designing a structural component.

Ponter [6] has examined the problem of thermal loading in the absence of creep. His conclusions are best illustrated by considering the two bar structure of Fig. 1. The two bars are constrained to deform axially by the same amount under the influence of a constant load P whilst the temperature of the thicker bar is oscillated between θ_{min} and θ_0 and that of the thinner bar is oscillated between θ_{min} and $\theta_0 + \Delta\theta$. Under this thermal loading the maximum thermo-elastic stress occurs in the thinner bar at the temperature $\theta_0 + \Delta\theta$. It is

$$\sigma_r = \tfrac{1}{8}E\alpha\Delta\theta.$$

Figure 2 shows the shakedown and ratchet boundaries for an elastic-perfectly plastic material and a material model that allows complete isotropic hardening in parts of the structure that suffer large variations of thermal stresses, in this instance the thinner bar. For higher levels of thermal loading the isotropic hardening model gives the most conservative estimate of the ratchet boundary. The boundary found from a set of experiments on a two bar structure of copper [6] falls between those predicted by the two material models, thus demonstrating that the assumption of perfectly plastic be-

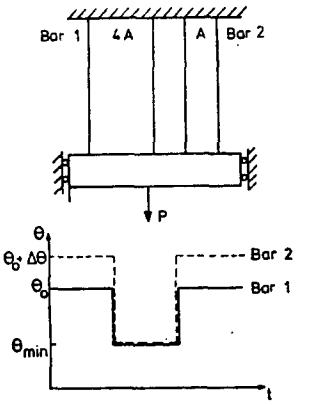

Fig. 1. Two bar structure subjected to a constant load P and cyclic variation of temperature.

haviour can be nonconservative. This may seem a rather surprising result since it is often assumed in structural analysis that it is safe to ignore the effects of hardening. The reason for this anomaly is that in thermal loading problems the assumption of perfect plasticity means that the range of stress is limited to $2\sigma_y$ (twice the yield stress) in regions of the structure that suffer large thermal strains. Because of equilibrium considerations the effect of this is to also limit the range of stress in the remainder of the structure, and as a result a larger primary load can be carried before yield is violated.

In [1] the same two bar structure was analysed for a material that suffers creep. Four different material models were considered:

(a) Non-linear viscous material.
(b) Non-linear viscous/perfectly plastic material.
(c) Isotropic hardening/recovery model.
(d) Isotropic hardening/recovery model with limiting yield surface.

For simplicity the following assumptions concerning the rate of loading and material properties were also made:

(i) Rapid cycling. That is when the cycle time is small compared with characteristic material times [7].

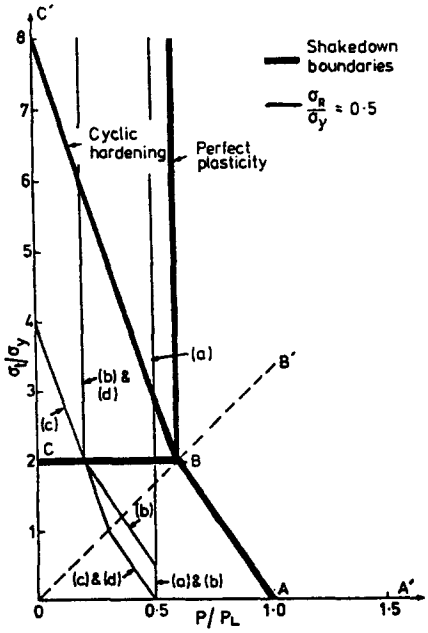

Fig. 2. Shakedown boundaries for two bar structure of Fig. 1. The thin lines represent contours of $\frac{\sigma_R}{\sigma_y} = 0.5$ for: (a) non-linear viscous material model; (b) non-linear viscous/perfectly plastic material model; (c) recovery model; (d) recovery model with limiting yield stress.

(ii) θ_{min} is outside of the creep range.
(iii) The creep properties over to temperature range θ_0 to $\theta_0 + \Delta\theta$ are independent of temperature and can be expressed in the form

$$\frac{\dot{\epsilon}}{\dot{\epsilon}_0} = \left(\frac{\sigma}{\sigma_0}\right)^n \tag{1}$$

where $\dot{\epsilon}_0$ is the strain rate at a constant stress σ_0.

The constant uniaxial stress that leads to a strain rate equal to that experienced by the two bars is defined as the reference stress, σ_R. Contours of constant reference stress predicted by the four material models are shown in Fig. 2. The combination of cyclic hardening and recovery of the flow stress during the high temperature part of the cycle leads to the most severe result. It is this material model that will be analysed in detail in the present paper.

The upper bound used in [1] ceases to be of any practical use when reversed plastic straining takes place in the structure. This is because the bound is presented in terms of total energy dissipated, and no distinction is made between the energy that is dissipated as a result of reversed straining and that which is dissipated as a result of the net deformation of an element of material. In the next section an alternative, yet more restrictive, bound is derived that takes into account cyclic straining. The restriction lies in the fact that it is only a bound on the rapid cycle solution [8] and it can only be applied to certain types of thermal loading problems. As in all bounds based on energy dissipation only the overall deformation of the structure is bounded. It happens that for situations where it cannot be used the design problem is not one of global deformation but one of localised strain accumulation. For conditions of rapid cycling a lower bound can be found to the rate of accumulation of strain at any point in the structure.

2. STRUCTURAL BEHAVIOUR FOR HIGH LEVELS OF THERMAL LOADING

The response of a material element to any loading situation was discussed in [1] and [2] for the recovery model. Under rapid cycle conditions an element of material creeps at a rate determined by the maximum value of the effective stress, ϕ, experienced during the cycle.

$$\dot{\epsilon}_{ij} = \frac{\dot{\epsilon}_0}{\sigma_0^n} \phi_{max}^n \frac{\partial\phi}{\partial\sigma_{ij}} \int_0^1 \exp[\gamma(\theta - \theta_0)]\, d\tau \tag{2}$$

where $\tau = \frac{t}{t_c}$, t is the time into the cycle and t_c is the cycle time. The quantity γ is defined as

$$\gamma = \frac{\Delta H}{R\theta_0^2}$$

where ΔH is the activation energy for creep, R is the universal gas constant and θ_0 is a reference temperature.

Here we are going to examine structural situations where the thermal loading is cycled between two prescribed limits. Then if ϕ is the same at both ends of the cycle the overall strain rate is

$$\dot{\epsilon}_{ij} = \frac{\dot{\epsilon}_0}{\sigma_0^n} \phi^n \left\{\int_0^1 \exp[\gamma(\theta - \theta_0)]\, d\tau\right\} \cdot \left[\eta \frac{\partial\phi}{\partial\sigma_{ij}^1} + (1 - \eta) \frac{\partial\phi}{\partial\sigma_{ij}^2}\right] \tag{3}$$

where σ_{ij}^1 and σ_{ij}^2 are the stresses at the two ends of the cycle and η takes a value between 0 and 1. η is not related to the cycle time but is determined from the compatibility requirement of the entire structure [9].

When considering the possibility of reversed plastic straining it proves advantageous to write the stress at a point in the form

$$\sigma_{ij} = \sigma_{ij}^{p} \pm \frac{\Delta\hat{\sigma}_{ij}^{\theta}}{2} \tag{4}$$

where σ_{ij}^{p} is the stress distribution in equilibrium with the primary load P_i and $\Delta\hat{\sigma}_{ij}^{\theta}$ is the range of thermo-elastic stress at that point. Choosing an equilibrium stress field,

$$\sigma_{ij}^{*} = \sigma_{ij}^{*P} + \sigma_{ij}^{*T} \tag{5}$$

where σ_{ij}^{*P} is a stress field in equilibrium with P_i and σ_{ij}^{*T} is in equilibrium with a dummy load T_i applied in the direction of the required displacement rate, such that

$$\sigma_{ij}^{*} \cdot \Delta\hat{\sigma}_{ij}^{\theta} = 0 \tag{6}$$

in a volume V_F^* of the structure, it is shown in the Appendix that the deformation rate is bounded by

$$\int_{S_T} T_i \dot{u}_i \, dS \leqslant \frac{\dot{\epsilon}_0}{n\sigma_0^n} \left\{ \int_{V_s^*} \phi_{\max}^{n+1} \left[\frac{n}{n+1} \left(\sigma_{ij}^{*} \pm \frac{\Delta\hat{\sigma}_{ij}^{\theta}}{2} \right) \right] \left[\int_0^1 e^{\gamma(\theta-\theta_0)} \, d\tau \right] dV \right.$$
$$\left. + \int_{V_F^*} \phi^{n-1} \left(\frac{n}{n+1} \sigma_{ij}^{*} + \frac{\Delta\hat{\sigma}_{ij}^{\theta}}{2} \right) \cdot \phi^2 \left(\frac{n}{n+1} \sigma_{ij}^{*} \right) \left[\int_0^1 e^{\gamma(\theta-\theta_0)} \, d\tau \right] dV \right\} \tag{7}$$

for a von Mises material under rapid cycle loading conditions. V_s^* is that volume of the structure remaining after V_F^* has been removed. $\phi_{\max}\left[\frac{n}{n+1}\left(\sigma_{ij}^{*} \pm \frac{\Delta\hat{\sigma}_{ij}^{\theta}}{2}\right)\right]$ is the maximum value out of $\phi\left[\frac{n}{n+1}\left(\sigma_{ij}^{*} + \frac{\Delta\hat{\sigma}_{ij}^{\theta}}{2}\right)\right]$ and $\phi\left[\frac{n}{n+1}\left(\sigma_{ij}^{*} - \frac{\Delta\hat{\sigma}_{ij}^{\theta}}{2}\right)\right]$.

In the Appendix it is shown that the bound is only valid if the stress field σ_{ij}^{*} is chosen such that $\phi\left(\frac{n}{n+1}\sigma_{ij}^{*} + \frac{\Delta\hat{\sigma}_{ij}^{\theta}}{2}\right)$ has the minimum possible value in the volume V_F^*. It is not always possible to find a stress distribution that satisfies this condition and is also in equilibrium with P_i and T_i. This puts a limitation to the range of problems for which the bound can be employed.

Ponter [6] has identified two categories of structural behaviour below the creep range. The difference between the two types of behaviour lies in the ability of a structure to redistribute stress. In category A structures the primary load can be completely shed from regions that suffer large cyclic thermal stresses. These regions then experience reversed cyclic plastic strains and the structure can shakedown plastically. This type of behaviour is evidenced by the existence of a reversed plasticity region on the Bree diagram.

If from general equilibrium considerations components of the applied load must be transmitted through the volume of material that suffers large cyclic thermal stresses then no reversed plasticity region exists on the Bree diagram. Ratchetting takes place at all points outside of the elastic shakedown boundary. This type of structural behaviour belongs to the second category, category B. For low levels of primary load the ratchet mechanism is one of local accumulation of plastic strain.

In the following two sections it is shown that these classifications of structural behaviour apply equally well in the creep range. For category A structures it is always possible to use the bound of eqn (7), but for category B structures the bound can only be used in a small number of instances.

3. CATEGORY A STRUCTURES

Ponter [6] has shown that in the absence of creep a structure will shakedown if an arbitrary stress field exists such that

$$\sigma_{ij}^{*P} = 0 \tag{8}$$

in a region V_F of the structure, where V_F is the volume within which

$$\Delta\phi(\hat{\sigma}_{ij}^{\theta}) \geqslant 2\sigma_y \tag{9}$$

and

$$\phi_{\max}\left(\sigma_{ij}^{*P} \pm \frac{\Delta\hat{\sigma}_{ij}^{\theta}}{2}\right) \leqslant \sigma_y \tag{10}$$

in the remainder of the structure.

The plastic shakedown boundary is then given by an equation of the form

$$\sigma_y = f(P, \sigma_t) \tag{11}$$

where $f(P, \sigma_t)$ is a function of the primary load P and maximum thermo-elastic stress σ_t.

For arbitrary values of P and σ_t an equilibrium stress field is given by eqns (8)–(10) with σ_y replaced by σ_R, where

$$\sigma_R = f(P, \sigma_t).$$

If a stress distribution can also be found such that

$$\sigma_{ij}^{*T} = 0$$

in $V_F^* = V_F$, then

$$\phi\left(\frac{n}{n+1}\sigma_{ij}^{*} + \frac{\Delta\sigma_{ij}^{\theta}}{2}\right) = \phi\left(\frac{\Delta\sigma_{ij}^{\theta}}{2}\right)$$

in V_F^*, which is the minimum possible value there, and the bound, eqn (7) can be used. Because of this choice of stress distribution the integral over the volume V_F^* in eqn (7) is zero and we need only consider the remaining volume V_s^*. The bound now reduces to that used in [1], but applied to a reduced volume, V_s^*.

In [1] shakedown solutions were used that assumed a variation of yield stress through the structure. In many problems this is an unnecessary refinement and the use of a yield stress that is constant is accurate enough for use in design.

A situation that is typical of category A structures is the plate problem first analysed by Bree [10]. The loading situation is shown in Fig. 3 along with the thermo-elastic stress distribution. The resulting shakedown boundaries are shown in Fig. 4. When $\sigma_t \geqslant 2\sigma_y$ the plastic shakedown boundary is given by [6, 10]

$$\sigma_y = \sqrt{\sigma_p \sigma_t}. \tag{12}$$

The equilibrium stress field at a point on the boundary given by Ponter [6], who allows cyclic hardening at the outside of the plate, is shown in Fig. 5. The outer edges of the plate only carry the thermal load whilst the central region also supports the primary load, σ_y being the maximum stress it experiences during the cycle.

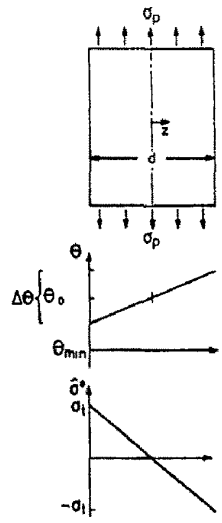

Fig. 3. Temperature and thermo-elastic stress distribution for Bree plate.

For any loading situation in the region C'COBB' of the Bree diagram an equilibrium stress field is

$$\phi_{\max}\left(\sigma_{ij}^{*P} \pm \frac{\Delta\hat{\sigma}_{ij}^{\theta}}{2}\right) = \sigma_R$$

for

$$-\frac{a}{2} \leqslant z \leqslant \frac{a}{2}$$

and

$$\phi(\sigma_{ij}^{*P}) = 0$$

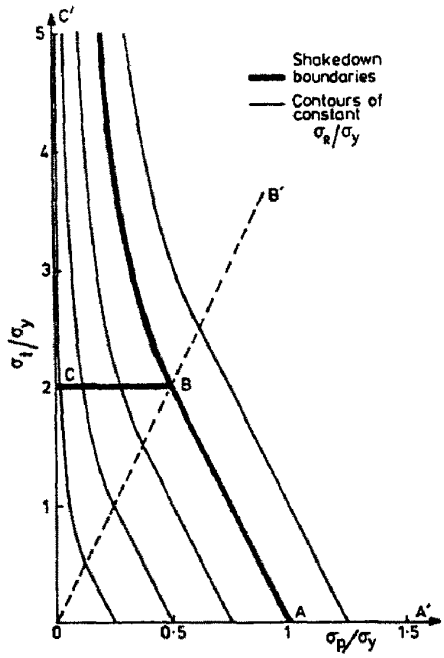

Fig. 4. Bree diagram showing contours of constant reference stress.

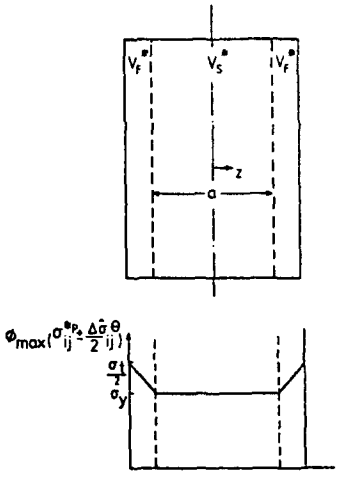

Fig. 5. Equilibrium stress field for a point on the plastic shakedown boundary in Fig. 4. V_F^* is the volume of material that experiences cyclic plastic strains.

for

$$\frac{a}{2} \leqslant |z| \leqslant \frac{d}{2}$$

where

$$\sigma_R = \sqrt{\sigma_p \sigma_t} \tag{13}$$

and

$$a = \frac{2\sigma_R}{\sigma_t} \cdot d.$$

If σ_{ij}^{*T} is selected such that

$$\phi(\sigma_{ij}^{*T}) = \beta\sigma_R$$

when

$$-\frac{a}{2} \leqslant z \leqslant \frac{a}{2}$$

and

$$\phi(\sigma_{ij}^{*T}) = 0$$

when

$$\frac{a}{2} \leqslant |z| \leqslant \frac{d}{2}$$

then substitution of the above eqns into the bound, eqn (7), and optimizing *w.r.t.* β gives

$$\beta = \frac{1}{n}$$

and

$$\frac{\dot{u}}{l} \leqslant \frac{\dot{\epsilon}_0}{\sigma_0 n} \sigma_R^n \int_{-1/2}^{1/2} \left\{ \lambda \exp\left(\gamma \Delta\theta_t \frac{z}{a}\right) + (1 - \lambda) \exp[\gamma(\theta_{\min} - \theta_0)] \right\} \mathrm{d}\left(\frac{z}{a}\right)$$

where l is the length of plate and λ is the portion of the cycle spent at the higher temperature. The temperature $\Delta\theta_t$ is defined as

$$\Delta\theta_t = \frac{2\sigma_R}{\sigma_t} \cdot \Delta\theta = \frac{4\sigma_R}{E\alpha}. \tag{15}$$

Following the procedure used in [1] we define a reference material test conducted at constant stress σ_R and cyclic temperature history. The temperature being oscillated between θ_R and $\theta_{\min}$, where θ_R is maintained for a fraction λ of the cycle and is defined as $\theta_R = \theta_0 + x\Delta\theta_t$. The resulting mean strain rate in such a test is

$$\dot{\epsilon}_R = \frac{\dot{\epsilon}_0}{\sigma_0^n} \sigma_R^n \{\lambda \exp(\gamma x \Delta\theta_t) + (1 - \lambda) \exp[\gamma(\theta_{\min} - \theta_0)]\}.$$

If we define θ_R so that

$$\frac{u}{l} \leqslant \dot{\epsilon}_R$$

then, from eqns (14)–(16), the reference temperature is given by

$$x = \frac{E\alpha}{4\gamma\sigma_R} \ln\left[\frac{E\alpha}{2\gamma\sigma_R} \sinh\left(\frac{2\gamma\sigma_R}{E\alpha}\right)\right].$$

For small values of $\frac{2\gamma\sigma_R}{E\alpha}$ this reduces to

$$x = \frac{1}{12} \frac{\sigma_R \gamma}{E\alpha}. \tag{17}$$

In most practical situations the value of x given by eqn (17) is small and it is sufficient to let $\theta_R = \theta_0$, the mean temperature of the plate.

Contours of constant reference stress σ_R given by eqn (13) are plotted on Fig. 4 along with the results for low levels of thermal loading [1]. For category A type structures the shape of the σ_R contours is given by the equation for the plastic shakedown boundary with σ_y replaced by σ_R. The deformation rate of the structure can be related to the strain rate in a uniaxial test at constant stress, σ_R, and cyclic temperature between θ_0 and $\theta_{\min}$.

A comparison of the results given here and in [1] with those given by O'Donnell and Porowski [11] is given in Section 5.

4. CATEGORY B STRUCTURES

Two structural problems that fall into this category of behaviour are shown in Figs. 6 and 8. Ponter [6] has analysed the plastic deformation of these structures in the absence of creep.

The first situation considered here is that of a temperature front oscillating over a small portion of tube, Fig. 6. The shakedown boundaries for this problem are shown

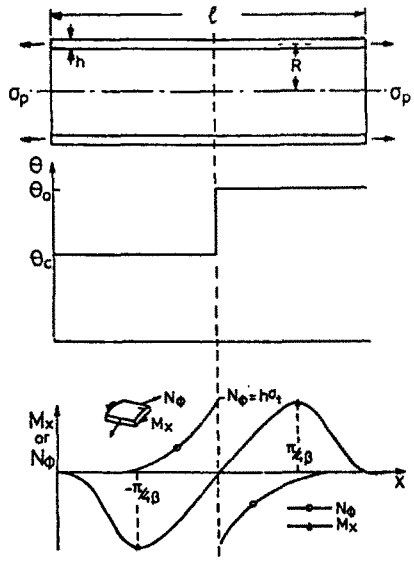

Fig. 6. Thermo-elastic stress distribution in the vicinity of a temperature front that moves along the tube.

in Fig. 7. Beyond AB the mode of plastic incremental collapse is overall axial extension of the tube. While beyond CB the tube deforms by a local thinning and extension in the region of oscillation of the temperature front.

The creep deformation for loading situations in the region A'AOBB' of the Bree diagram was analysed in [1]. In the next sub-section we apply the bound of eqn (7) to the region C'COBB'. The result is a bound on the overall axial deformation rate. Use of the bound gives no information about the local accumulation of strain in the structure. It is shown that in design the local accumulation of strain is the most important aspect of structural behaviour, as it is at low temperature. An estimate of the rate of accumulation of strain in the region of oscillation of the temperature front is given.

In sub-section 4.2, it is shown that the bound cannot be used for the problem of a plate supporting a normal pressure, Fig. 8, for high levels of thermal loading. This is not a great drawback since, as in the tube problem, it is the rate of accumulation of strain in regions that suffer high levels thermal loading that is important in design.

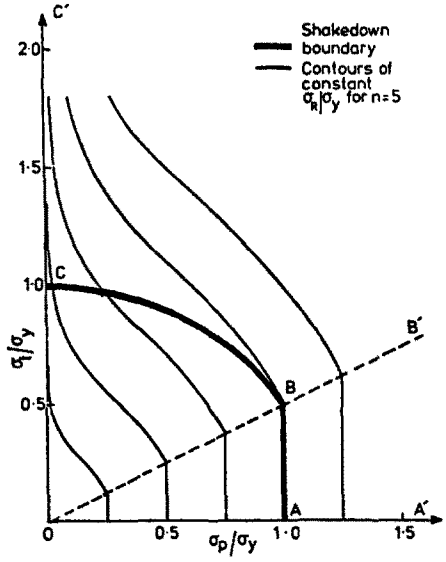

Fig. 7. Bree diagram for short travel problem showing contours of constant reference stress.

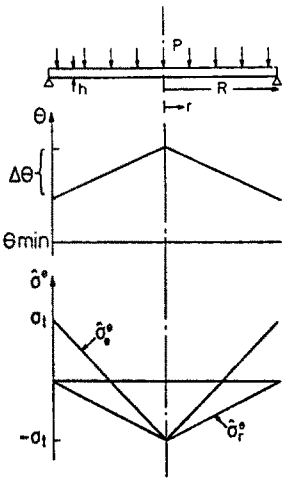

Fig. 8. Thermo-elastic stress distribution in simply supported circular plate for temperature distribution shown.

4.1. *Temperature front moving along a tube—short travel problem*

Over the region where the temperature front oscillates the range of thermal loading is

$$\Delta\hat{\sigma}^{\theta}_{\phi} = 2\sigma_t$$

$$\Delta\hat{\sigma}^{\theta}_{R} = \Delta\hat{\sigma}^{\theta}_{a} = 0$$

where

$$\sigma_t = \frac{E\alpha\Delta\theta}{2}$$

and the subscripts ϕ, R and a denote hoop, radial and axial components respectively. Outside this region the range of thermal loading is practically zero.

Any annular element of material must transmit the axial stress σ_p. So the only stress that can redistribute is the hoop component and we find that in the region of oscillation of the temperature front the minimum possible value of ϕ is

$$\phi_{\min} = (\tfrac{3}{4}\sigma_p^2 + \sigma_t^2)^{1/2} \tag{18}$$

and the resulting residual hoop component of stress is

$$\sigma^R_{\phi} = \frac{\sigma_p}{2}$$

this must be balanced by a distribution of hoop stress in the remainder of the tube. But if the tube is sufficiently long then this additional stress can be safely ignored. Selection of $\sigma^{*T} = \frac{1}{n}\sigma_p$ where σ^{*T} is the axial stress resulting from application of the dummy load, permits the choice

$$\phi\left(\frac{n}{n+1}\sigma^*_{ij} + \frac{\Delta\hat{\sigma}^{\theta}_{ij}}{2}\right) = \phi_{\min}$$

in V^*_F, where V^*_F is the volume over which the temperature front moves, and

$$\phi_{\max}\left[\frac{n}{n+1}\left(\sigma^*_{ij} \pm \frac{\Delta\hat{\sigma}^{\theta}_{ij}}{2}\right)\right] = \sigma_p$$

in the remainder of the tube. The bound then becomes

$$\dot{u} \leqslant \frac{\dot{\epsilon}_0}{\sigma_0^n} \langle l_c \sigma_p^n \exp[\gamma(\theta_c - \theta_0)] + l_h \sigma_p^n + \tfrac{3}{4} l_0 \sigma_p (\tfrac{3}{4}\sigma_p^2 + \sigma_t^2)^{\frac{n-1}{2}} \{\lambda + (1 - \lambda) \exp[\gamma(\theta_c - \theta_0)]\}\rangle \quad (19)$$

where l_c is the length of tube always subjected to the lowest temperature, θ_c, l_h is the length at the highest temperature, θ_0 and l_0 is the length of tube over which the temperature front oscillates. In deriving eqn (19) it was assumed that the temperature front moves very fast and remains stationary for a time at both extremes of the cycle. λ is that fraction of the cycle when l_0 experiences the high temperature.

Unless the tube is short, eqn (19) shows that the overall deformation rate of the tube is not very sensitive to the presence of the temperature front. For this type of problem it is not the overall deformation of the structure, but the accumulation of strain locally, that is limiting in design. For this particular problem the ring of material over which the temperature front moves must transmit the axial load. Because of this we are able to calculate the minimum value of ϕ, eqn (18), and it follows that the rate of accumulation of effective strain locally is

$$\dot{\epsilon}_e \geqslant \frac{\dot{\epsilon}_0}{\sigma_0^n} (\tfrac{3}{4}\sigma_p^2 + \sigma_t^2)^{\frac{n-1}{2}} \sigma_p \{\lambda + (1 - \lambda) \exp[\gamma(\theta_c - \theta_0)]\} \quad (20)$$

under rapid cycle loading conditions. This is an unsafe bound but it gives us an idea of the behaviour of the structure. For large values of σ_t the local deformation rate is much greater than the mean rate.

If we define σ_R as

$$\sigma_R = (\tfrac{3}{4}\sigma_p^2 + \sigma_t^2)^{\frac{n-1}{2n}} \cdot \sigma_p^{1/n} \quad (21)$$

then

$$\dot{\epsilon}_e \geqslant \dot{\epsilon}_R$$

where

$$\dot{\epsilon}_R = \dot{\epsilon}_0 \{\lambda + (1 - \lambda) \exp[\gamma(\theta_c - \theta_0)]\} \quad (22)$$

is the strain rate in a uniaxial test at the constant stress σ_R when the temperature is cycled between θ_c and θ_0.

Contours of constant reference stress are plotted in Fig. 7 for $n = 5$.

4.2. *Plate supporting a normal pressure*

The loading situation for this problem is shown in Fig. 8. Each element of plate must transmit a shear stress

$$\tau = \frac{pr}{2h}$$

assuming that the shear stress is uniformly distributed through the thickness of the plate, h. As a result the minimum value of ϕ at any point is

$$\phi_{\min} = \left\{3\left(\frac{pr}{2h}\right)^2 + \left[1 - 3\frac{r}{R}\left(1 - \frac{r}{R}\right)\right]^2 \frac{\sigma_t^2}{4}\right\}^{1/2} \quad (23)$$

where

$$\sigma_t = \frac{E\alpha\Delta\theta}{3}.$$

Unless V_F^* is very small it is not possible to find a stress distribution such that $\phi\left(\frac{n}{n+1}\sigma_{ij}^* + \frac{\Delta\hat{\sigma}_{ij}^{\theta}}{2}\right)$ equals $\phi_{\min}$ and also satisfies equilibrium in V_F^*. The bound of eqn (7) cannot therefore be used for this problem.

For large values of the ratio σ_t/p we would expect the accumulation of strain in regions that suffer large variations of thermo-elastic stress to be the most critical feature of structural behaviour, as opposed to the overall deformation of the plate. When σ_t/p is large we can estimate the rate of accumulation of strain at the support in the following manner:

the outer ring of material must carry a shear stress

$$\tau = \frac{pR}{2h}$$

and because the stress cannot redistribute in this direction we find that strain accumulates at a rate

$$\dot{\epsilon} \geqslant \frac{\sqrt{3}\dot{\epsilon}_0}{2\sigma_0^n}\left[\frac{3}{4}\left(\frac{pR}{h}\right)^2 + \frac{\sigma_t^2}{4}\right]^{\frac{n-1}{2}}\frac{pR}{h}\{\lambda + (1-\lambda)\exp[\gamma(\theta_c - \theta_0)]\} \tag{24}$$

where θ_c is the uniform temperature when there is no temperature gradient across the plate and θ_0 is the temperature at the outside edge when there is a gradient.

If we define a reference stress, σ_R

$$\sigma_R = \left[\frac{3}{4}\left(\frac{pR}{h}\right)^2 + \frac{\sigma_t^2}{4}\right]^{\frac{n-1}{2n}}\left(\frac{\sqrt{3}pR}{2h}\right)^{1/n}$$

or in terms of the limit load

$$\sigma_R = \left[\frac{27}{16}\left(\frac{P}{P_L}\cdot\frac{h}{R}\right)^2 + \frac{1}{4}\left(\frac{\sigma_t}{\sigma_y}\right)^2\right]^{\frac{n-1}{2n}}\left(\frac{3\sqrt{3}pR}{4}\cdot\frac{P}{P_L}\cdot\frac{h}{R}\right)^{1/n} \tag{25}$$

where

$$P_L = \frac{3}{2}\sigma_y\frac{h^2}{R^2}$$

then

$$\dot{\epsilon}_e \geqslant \dot{\epsilon}_R$$

where $\dot{\epsilon}_R$ is given by eqn (22).

Contours of constant reference stress are plotted in Fig. 9 for $n = 5$ and $\frac{h}{R} = \frac{1}{10}$.

At the present time we are unable to find expressions for the deformation of the plate in the region DOB of the Bree diagram. This must await the development of a more general bound for instances of cyclic straining or the production of exact numerical results.

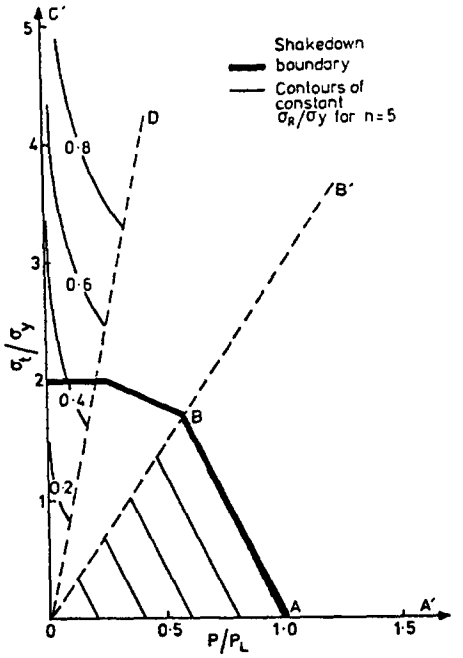

Fig. 9. Bree diagram for simply supported plate showing contours of constant reference stress.

The line OD has been drawn in an arbitrary position in Fig. 9 since the range of applicability of eqn (25) is unknown at the present time.

5. DISCUSSION

In [1] upper bounds to the deformation rate of structures subjected to low levels of thermal loading were given. Stress distributions resulting from low temperature shakedown analyses were used to facilitate the production of these bounds. Here these results have been extended to high levels of thermal loading through the use of a bound on the rapid cycle solution that takes into account reversed cyclic strains during a loading cycle.

Ponter [6] has identified two types of structural behaviour in the absence of creep effects. It has been shown here that these classifications of structural behaviour apply equally well when deformation due to creep becomes important. Problems typical of the different classes have been analysed in Sections 3 and 4.

In Section 3 an upper bound is given for the Bree problem [10] which is typical of the behaviour of category A type structures. The deformation rate is related to the strain rate of a uniaxial specimen subjected to a constant reference stress, σ_R, and a temperature that is cycled between θ_0, the mean temperature in the plate, and θ_{min}. Contours of

$$\frac{\sigma_R}{\sigma_y} = 0.5$$

predicted by the present analysis and by O'Donnell and Porowski [11] for a non-linear viscous/perfectly plastic material under rapid cycle conditions are compared in Fig. 10. In their analysis it was assumed that θ_{min} is outside of the creep range and that the creep properties at the high temperature end of the cycle are independent of temperature. Although O'Donnell and Porowski [11] do not mention a reference temperature the choice of a temperature that is cycled between θ_0 and θ_{min} in the reference test is consistent with their analysis.

From Fig. 10 it can be seen that the present analysis leads to the more conservative result. The experimental results of Megahed, Ponter and Morrison [3, 4] also vindicate

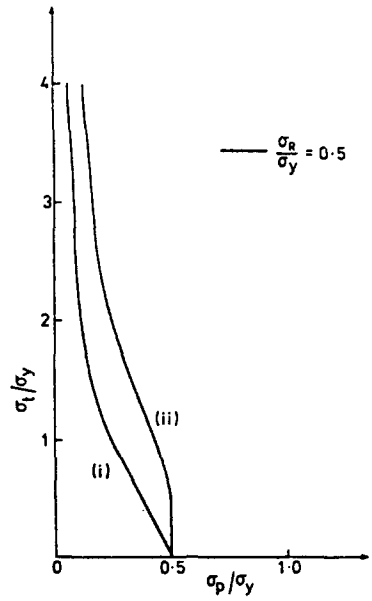

Fig. 10. Contours representing $\frac{\sigma_R}{\sigma_y} = 0.5$ for: (i) recovery model; (ii) non-linear viscous/perfectly plastic material model.

the use of the recovery model. If the difference between θ_0 and θ_{min} is large then we might expect the results predicted by the recovery model to be over conservative, as the variation of flow stress with temperature has not been included in the analysis. The recovery model can be easily ammended to take into account this temperature sensitivity of the flow stress. Cocks and Ponter [12] discuss the application of this modified model to thermal loading problems. The resulting reference stress lies between the two results of Fig. 10.

The bound developed here has only limited application for category B type structures. For this class, however, it is not the overall deformation of the structure, but the accumulation of strain in parts of the structure that suffer large thermal stresses that is limiting in design for high levels of thermal loading. Estimates of the rate of accumulation of strain in these highly stressed regions are given in Section 4. Because this local deformation is not constrained in the examples considered here (it is through thickness strain) the ASME design codes [13] classify it as a primary strain. As a result the total accumulation of strain is limited to 1% and not 5%, as it is for a secondary strain.

Acknowledgement—This work was supported by a grant from the Science and Engineering Research Council of Great Britain.

REFERENCES

1. A. C. F. Cocks and A. R. S. Ponter, Cyclic thermal loading in the creep range—I. Low levels of thermal loading. *Int. J. Solids Structures* **21**, 187 (1985).
2. A. R. S. Ponter and F. A. Leckie, Constitutive relationships for the time-dependent deformation of metals. *J. Engng Mat. Tech.* **98**, 47 (1976).
3. M. M. Megahed and A. R. S. Ponter, Creep and plastic ratchetting in cyclically thermally loaded structures. *IUTAM* Symposium on Physical Non-Linearities in Structural Analysis, (edited by J. Hult and J. Lemaitre), pp. 220–227. Springer-Verlag, Berlin (1981).
4. M. M. Megahed, A. R. S. Ponter and C. J. Morrison, An experimental and theoretical investigation into the creep properties of a simple structure of 316 stainless steel. Leicester University Engineering Department Report 82-7 (1982).
5. J. L. Chaboche and G. Rousselier, On the plastic and viscoplastic constitutive equations based on the internal variable concept. 3rd International Seminar on Inelastic Analysis and Life Prediction in High Temperature Environment, Paris (1981).
6. A. R. S. Ponter, Shakedown and ratchetting below the creep range. Part II theoretical considerations. Leicester University Engineering Department Report 81-13 (1981).

7. A. R. S. Ponter, Deformation, displacement and work bounds for structures in a state of creep and subject to variable loading. *J. Appl. Mech.* **39**, 953 (1972).
8. A. R. S. Ponter, Deformation bounds for the Bailey-Orowan theory of creep. *J. Appl. Mech.* **42**, 619 (1975).
9. A. C. F. Cocks and A. R. S. Ponter, The plastic behaviour of components subjected to constant primary stresses and cyclic secondary strains. To appear in *J. Strain Analysis*.
10. J. Bree, Elastic-plastic behaviour of thin tubes subjected to internal pressure and intermittent high-heat fluxes with application to fast-nuclear-reactor fuel elements. *J. Strain Analysis* **2**, 226 (1967).
11. W. J. O'Donnell and J. S. Porowski, Upper bound for accumulated strains due to creep ratchetting. Welding Research Council Bulletin No. 185 (1974).
12. A. C. F. Cocks and A. R. S. Ponter, to be published.
13. ASME Boiler and Pressure Vessel Code, Code Case N-47.
14. R. Hill, New horizons in the mechanics of solids. *J. Mech. Phys. Solids* **5**, (1956).
15. A. R. S. Ponter, Energy theorems and deformation bounds for constitutive relations associated with creep and plastic deformation of metals. *J. Mech. Phys. Solids* **17**, 493 (1969).

APPENDIX

Upper bound to rapid cycle solution

Under rapid cycle loading conditions an element of material creeps according to eqns (2) and (3). If under constant loading conditions an element of material creeps at a rate

$$\dot{\epsilon}_{ij} = \frac{\dot{\epsilon}_0}{\sigma_0^n} \phi^n \frac{\partial \phi}{\partial \sigma_{ij}} \int_0^1 \exp \gamma(\theta - \theta_0)\, d\tau \tag{A1}$$

we can write the convexity condition [14, 15]

$$\sigma_{ij}^a \dot{\epsilon}_{ij}^b - \frac{n}{n+1} \sigma_{ij}^b \dot{\epsilon}_{ij}^b \leqslant \frac{1}{n+1} \sigma_{ij}^a \dot{\epsilon}_{ij}^a \tag{A2}$$

where σ_{ij}^a and σ_{ij}^b are any two stress states and $\dot{\epsilon}_{ij}^a$ and $\dot{\epsilon}_{ij}^b$ are the resulting respective strain rates given by eqn (A1).

Fig. A1(a) shows a structure subjected to a constant primary load, P_i, and cyclic thermal loading such that the actual stress state in the structure is

$$\sigma_{ij} = \sigma_{ij}^p \pm \frac{\Delta \hat{\sigma}_{ij}^\theta}{2}.$$

Now consider the same structure subjected to a constant load $\frac{n}{n+1}(P_i + T_i)$ and $\frac{n}{n+1}\sigma_{ij}^* = \frac{n}{n+1}(\sigma_{ij}^{*P} + \sigma_{ij}^{*T})$ is any stress field in equilibrium with $\frac{n}{n+1}(P_i + T_i)$, Fig. A1(b). The volume of the structure where our choice of σ_{ij}^* is such

$$\phi\left(\frac{n}{n+1}\sigma_{ij}^* + \frac{\Delta \hat{\sigma}_{ij}^\theta}{2}\right) = \phi\left(\frac{n}{n+1}\sigma_{ij}^* - \frac{\Delta \hat{\sigma}_{ij}^\theta}{2}\right) \tag{A3}$$

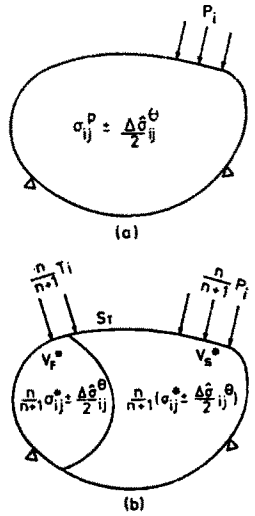

Fig. A1. (a) Structure subjected to constant primary load P_i and cyclic variation of temperature. (b) Stress distributions used in bound.

will be termed V_F^*. For a von Mises material a consequence of eqn (A3) is that

$$\sigma_{ij}^* \cdot \Delta\hat{\sigma}_{ij}^\theta = 0 \tag{A4}$$

in this region.

We will term the remainder of the structure V_s^*. These two volumes can now be examined separately.

The volume V_s^*

If σ_{ij}^p is identified with the actual stress distribution, σ_{ij}, and σ_{ij}^a is set equal to

$$\sigma_{ij}^a = \frac{n}{n+1}\sigma_{ij}^* \pm \frac{n}{n+1}\frac{\Delta\hat{\sigma}_{ij}^\theta}{2}$$

the convexity condition, eqn (A2) can be used at each end of the cycle:

$$\begin{aligned}
&\frac{n}{n+1}\sigma_{ij}^*\dot{\epsilon}_{ij}^1 - \frac{n}{n+1}\sigma_{ij}^p\dot{\epsilon}_{ij}^1 \\
&\quad \leqslant \frac{1}{n+1}\frac{\dot{\epsilon}_0}{\sigma_0^n}\phi^{n+1}\left[\frac{n}{n+1}\left(\sigma_{ij}^* + \frac{\Delta\hat{\sigma}_{ij}^\theta}{2}\right)\right]\cdot\int_0^1 \exp\gamma(\theta-\theta_0)\,d\tau \\
&\frac{n}{n+1}\sigma_{ij}^*\dot{\epsilon}_{ij}^2 - \frac{n}{n+1}\sigma_{ij}^p\dot{\epsilon}_{ij}^2 \\
&\quad \leqslant \frac{1}{n+1}\frac{\dot{\epsilon}_0}{\sigma_0 n}\phi^{n+1}\left[\frac{n}{n+1}\left(\sigma_{ij}^* - \frac{\Delta\hat{\sigma}_{ij}^\theta}{2}\right)\right]\cdot\int_0^1 \exp\gamma(\theta-\theta_0)\,d\tau
\end{aligned} \tag{A5}$$

where $\dot{\epsilon}_{ij}^1$ is the strain rate given by eqn (A1) for a stress

$$\sigma_{ij} = \sigma_{ij}^p + \frac{\Delta\hat{\sigma}_{ij}^\theta}{2}$$

and $\dot{\epsilon}_{ij}^2$ is the resulting strain rate for

$$\sigma_{ij} = \sigma_{ij}^p - \frac{\Delta\hat{\sigma}_{ij}^\theta}{2}.$$

The *r.h.s.* of eqns (A5) results from the use of eqn (A1) for $\dot{\epsilon}_{ij}^a$ and noting that

$$\sigma_{ij}\frac{\partial\phi}{\partial\sigma_{ij}} = \phi.$$

If the first of eqns (A5) is multiplied by η and the second by $(1-\eta)$, where η is that fraction of $\dot{\epsilon}_{ij}^1$ that contributes to the overall strain rate of the element of material, we find after combining the two equations that

$$\begin{aligned}
\frac{n}{n+1}(\sigma_{ij}^* - \sigma_{ij}^p)\dot{\epsilon}_{ij} &\leqslant \frac{1}{n+1}\frac{\dot{\epsilon}_0}{\sigma_0^n}\left\{\eta\phi^{n+1}\left[\frac{n}{n+1}\left(\sigma_{ij}^* + \frac{\Delta\hat{\sigma}_{ij}^\theta}{2}\right)\right] + (1-\eta)\phi^{n+1}\right. \\
&\quad \left.\times\left[\frac{n}{n+1}\left(\sigma_{ij}^* - \frac{\Delta\hat{\sigma}_{ij}^\theta}{2}\right)\right]\right\}\cdot\int_0^1 \exp\gamma(\theta-\theta_0)\,d\tau \\
&\leqslant \frac{1}{n+1}\frac{\dot{\epsilon}_0}{\sigma_0^n}\phi_{\max}^{n+1}\left[\frac{n}{n+1}\left(\sigma_{ij}^* \pm \frac{\Delta\hat{\sigma}_{ij}^\theta}{2}\right)\right]\cdot\int_0^1 \exp\gamma(\theta-\theta_0)\,d\tau
\end{aligned} \tag{A6}$$

where

$$\dot{\epsilon}_{ij} = \eta\dot{\epsilon}_{ij}^1 + (1-\eta)\dot{\epsilon}_{ij}^2$$

is the overall strain rate of the element of material, see eqn (3), and $\phi_{\max}\left[\frac{n}{n+1}(\sigma_{ij}^* \pm \Delta\hat{\sigma}_{ij}^\theta/2)\right]$ is the maximum value of $\phi\left[\frac{n}{n+1}(\sigma_{ij}^* + \Delta\hat{\sigma}_{ij}^\theta/2)\right]$ and $\phi\left[\frac{n}{n+1}(\sigma_{ij}^* - \Delta\hat{\sigma}_{ij}^\theta/2)\right]$.

The volume V_F^*

Application of the convexity condition to each end of the cycle using the stress states

$$\sigma_{ij}^b = \sigma_{ij}$$

and

$$\sigma_{ij}^a = \frac{n}{n+1}\sigma_{ij}^* \pm \frac{\Delta\hat{\sigma}_{ij}^\theta}{2}$$

leads to the result

$$\frac{n}{n+1}(\sigma_{ij}^{*}-\sigma_{ij}^{\theta})\dot{\epsilon}_{ij} \leqslant \frac{1}{n+1}\frac{\dot{\epsilon}_0}{\sigma_0^n}\phi^{n-1}\left(\frac{n}{n+1}\sigma_{ij}^{*}+\frac{\Delta\hat{\sigma}_{ij}^{\theta}}{2}\right)\cdot\phi^2\left(\frac{n}{n+1}\sigma_{ij}^{*}\right)\int_0^1 \exp\gamma(\theta-\theta_0)\,d\tau$$

$$+\frac{1}{n+1}\frac{\dot{\epsilon}_0}{\sigma_0^n}\left[\phi^{n-1}\left(\frac{n}{n+1}\sigma_{ij}^{*}+\frac{\Delta\hat{\sigma}_{ij}^{\theta}}{2}\right)-\phi_{\max}^{n-1}\left(\sigma_{ij}^{\theta}\pm\frac{\Delta\hat{\sigma}_{ij}^{\theta}}{2}\right)\right]\phi^2\left(\frac{\Delta\hat{\sigma}_{ij}^{\theta}}{2}\right)\cdot\int_0^1 \exp\gamma(\theta-\theta_0)\,d\tau. \quad \text{(A7)}$$

The stress $\phi_{\max}(\sigma_{ij}^{\theta}\pm\Delta\hat{\sigma}_{ij}^{\theta}/2)$ is not known, but if we select σ_{ij}^{*} such that $\phi\left(\frac{n}{n+1}\sigma_{ij}^{*}+\Delta\hat{\sigma}_{ij}^{\theta}/2\right)$ has the minimum possible value in V_F^{*} we may write

$$\frac{n}{n+1}(\sigma_{ij}^{*}-\sigma_{ij}^{\theta})\dot{\epsilon}_{ij} \leqslant \frac{1}{n+1}\frac{\dot{\epsilon}_0}{\sigma_0^n}\phi^{n-1}\left(\frac{n}{n+1}\sigma_{ij}^{*}+\frac{\Delta\hat{\sigma}_{ij}^{\theta}}{2}\right)\cdot\phi^2\left(\frac{n}{n+1}\sigma_{ij}^{*}\right)\int_0^1 \exp\gamma(\theta-\theta_0)\,d\tau \quad \text{(A8)}$$

Integration of eqn (A6) over the volume V_x^{*} and of eqn (A8) over the volume V_F^{*} and application of the principle of virtual work leads to the result of eqn (7).